Published in final edited form as:
Cell Metab. 2012 July 3; 16(1): 81–89. doi:10.1016/j.cmet.2012.05.009.

Stamp2 controls macrophage inflammation through nicotinamide adenine dinucleotide phosphate homeostasis and protects against atherosclerosis

Henrik ten Freyhaus[1,4,*], **Ediz S. Calay**[1,*], **Abdullah Yalcin**[1], **Sara N. Vallerie**[1,5], **Ling Yang**[1], **Zerrin Z. Calay**[6], **Fahri Saatcioglu**[2], and **Gökhan S. Hotamisligil**[1,3]

[1]Departments of Genetics and Complex Diseases, Harvard School of Public Health, Boston, MA 02115, USA

[2]Molecular Biosciences, University of Oslo, Oslo, 0316, Norway

[3]Harvard-MIT Broad Institute, Cambridge, MA 02142, USA

[4]Klinik III für Innere Medizin, Universität zu Köln, Köln, 50937, Germany

[6]ETA Pathology and Cytology Lab, Istanbul, 34365, Turkey

Abstract

The six-transmembrane protein Stamp2 plays an important role in metabolically-triggered inflammation and insulin action. However, how and in which target cells Stamp2 regulates inflammatory responses and the physiological consequences remain unknown. Here we report that Stamp2 is expressed in human and mouse macrophages, is regulated upon differentiation or activation, acts as an anti-inflammatory protein, and regulates foam cell formation. Absence of Stamp2 results in significant increases in cellular NADPH levels, and both NADPH homeostasis and the exaggerated inflammatory response of Stamp2$^{-/-}$ macrophages are rescued by exogenous wild-type but not by a reductase-deficient Stamp2 molecule. Chemical and genetic suppression of NADPH production in Stamp2$^{-/-}$ macrophages restores the heightened inflammatory response. Stamp2 is detected in mouse and human atherosclerotic plaques and its deficiency promotes atherosclerosis in mice. Furthermore, bone marrow transplantation experiments demonstrated that Stamp2 in myeloid cells is sufficient to protect against atherosclerosis. Our data reveal a role of Stamp2 in controlling intermediary metabolites to regulate inflammatory responses in macrophages and in progression of atherosclerosis.

Address all correspondence to: Gökhan S. Hotamisligil, MD, PhD., 665 Huntington Av., Boston, MA 02115, ghotamis@hsph.harvard.edu Tel: 617 432 1950, Fax: 617 432 1941.
[5]Present address of SNV: Pacific Northwest Diabetes Res. Ins., Seattle, WA, 98119, USA
[*]These authors have contributed equally

INTRODUCTION

Metaflammation, the chronic, low-grade and metabolically orchestrated immune response at key metabolic organs including adipose tissue, is a hallmark of obesity and contributes to related complications such as insulin resistance and beta cell dysfunction (Eguchi et al., 2012; Hotamisligil, 2006; Schenk et al., 2008; Shoelson et al., 2006). Importantly, metabolic and inflammatory signals are tightly linked, and their coordinated action is important for the maintenance of metabolic homeostasis. This is best exemplified by the fact that both nutrients (such as glucose and lipids) and cytokines are able to activate inflammatory and stress signaling pathways like JNK, IKK, PKR, and others, leading to aberrant immune response, insulin resistance, beta cell dysfunction, metabolic dysregulation, and type 2 diabetes (Hotamisligil, 2006; Lumeng and Saltiel, 2011; Medzhitov, 2008). There are also intimate interactions between metabolic and immune effectors at sites critical for metabolic homeostasis, such as macrophages and adipocytes in adipose tissue, or Kuppfer cells and hepatocytes in liver, and many others, which are critical for metabolic regulation and chronic disease (Olefsky and Glass, 2010). Since, these cells also share many of the same molecules and networks that respond to nutrient- or pathogen-related signals, the proper function of this complex and highly integrated system requires proper control systems to maintain homeostasis, which are not well understood.

The impact of nutrients on inflammatory pathways demands the existence of counter-regulatory mechanisms to prevent overt inflammation or to mitigate stress upon physiological fluctuations in nutrient availability and transient surges at critical cells or organs. Recently, the six-transmembrane protein of prostate (Stamp)-2 was discovered as a potential molecule involved in such a role in adipose tissue (Wellen et al., 2007). Stamp2, also known as TNF-induced adipose-related protein (TIARP) or six-transmembrane epithelial antigen of prostate 4 (STEAP4), belongs to a family of six-transmembrane proteins, termed either the STAMP or STEAP family. Three of the four family members, including Stamp2, were recently characterized as reductases (Ohgami et al., 2006). Stamp2 is significantly regulated by fasting and feeding in visceral adipose tissue, and was demonstrated to be required for normal metabolic homeostasis. Despite higher baseline levels, the nutritional regulation of Stamp2 in visceral adipose tissue is defective in obese models and total body Stamp2 deficiency leads to severe inflammation of visceral white adipose tissue and recapitulates features of the metabolic syndrome (Wellen et al., 2007). These findings indicate a potential role for Stamp2 in the development of metabolic syndrome through its ability to integrate metabolic and inflammatory responses.

Stamp2 expression was recently shown to be increased in the joints and spleen of a mouse model of inflammatory arthritis (Inoue et al., 2009). In this model as well as in adipose tissue of human obese subjects, where basal expression level is regulated similar to mouse models, Stamp2 expression does, at least in part, co-localize or correlate with the macrophage marker CD68 (Arner et al., 2008). Stamp2 expression has also been detected in circulating monocytes, and expression levels were reduced in humans with metabolic syndrome compared to healthy controls. Furthermore, decreased Stamp2 expression in these cells was inversely correlated with carotid plaque formation as determined by ultrasonography (Wang et al., 2010). Hence, we postulated that Stamp2 may have a

regulatory role in macrophages and could contribute to atherosclerosis, in which macrophage inflammatory responses play a critical role. Here, we report that Stamp2 controls inflammatory responses in macrophages by regulating intermediary metabolism and that its deficiency accelerates atherosclerosis.

RESULTS

Role of Stamp2 in macrophage inflammatory responses

We first examined the expression and potential differentiation-dependent regulation of Stamp2 in macrophages. Under basal conditions, human monocytic THP-1 cells expressed very low amounts of Stamp2 protein. However, Stamp2 expression was time-dependently and robustly upregulated upon differentiation of cells with PMA, both at the mRNA and protein level (Fig. 1A–C). We next analyzed whether Stamp2 expression in macrophages was subject to regulation by inflammatory stimuli. We treated immortalized bone marrow-derived mouse macrophages with the toll-like receptor (TLR) agonists Lipopolysaccharide (LPS), Zymosan and Polyinosinic:polycytidylic acid (Poly I:C). All of these agents induced a strong increase of Stamp2 expression, both at the mRNA and protein levels (Fig. S1A–C). In parallel experiments with primary peritoneal macrophages from wild-type (WT) mice, treatment with TLR agonists again induced a substantial increase of Stamp2 expression both in mRNA and protein levels (Fig. 1D–F). These data show that Stamp2 is expressed in both mouse and human macrophages and exhibits strong positive regulation during differentiation and by inflammatory stimuli.

We then examined whether Stamp2 has a direct role in modulating the inflammatory response and analyzed expression of inflammatory cytokines in primary macrophages from Stamp2$^{-/-}$ and WT mice. In these experiments, we observed significantly greater induction of IL-6, MCP-1, IL-1β and TNF-α mRNA expression in Stamp2$^{-/-}$ macrophages compared to WT cells after LPS treatment (Fig. 1G, S1D–F). In line with these observations, LPS-induced secretion of IL-6, MCP-1, IL-1β and TNF-α into the culture medium was also significantly augmented in Stamp2$^{-/-}$ macrophages compared to WT cells (Fig. 1H, S1G–I). Earlier studies have shown impaired insulin action and glucose transport in Stamp2 knock-down adipocytes and in Stamp2$^{-/-}$ adipose tissue (Wellen et al., 2007). Since insulin resistance in macrophages has been implicated in enhanced stress responses in these cells (Han et al., 2006), we examined insulin-induced Akt phosphorylation. However, we detected no differences in the insulin responsiveness of Stamp2$^{-/-}$ and WT macrophages (Fig. S1 J–K). Taken together, macrophages lacking Stamp2 expression are prone to an enhanced inflammatory response, but unlike adipocytes, they do not exhibit decreased insulin sensitivity.

Mechanisms underlying the overt inflammatory phenotype of Stamp2 deficiency

Expression of inducible nitric oxide synthase (iNOS) increases during macrophage activation. As shown in Fig. 2A–C, iNOS mRNA and protein expression were enhanced to a significantly greater extent in Stamp2$^{-/-}$ macrophages compared to WT cells upon treatment with LPS. In this setting, LPS-induced cellular release of NO into the culture medium was significantly higher in Stamp2-deficient macrophages (Fig. 2D). This led us consider NO

production by iNOS as a mechanism by which Stamp2 regulates inflammatory responses. We treated Stamp2-deficient macrophages with a highly iNOS-specific inhibitor W1400 (Fedorov et al., 2003). Interestingly, inhibition of iNOS had no effect on LPS-induced expression of IL-6 in Stamp2$^{-/-}$ and WT macrophages (Fig. 2E), illustrating that the changes in iNOS expression cannot account for the enhanced inflammatory response in Stamp2$^{-/-}$ macrophages.

This lead us to examine causality of defective Stamp2 function for the pro-inflammatory phenotype seen in macrophages by re-introducing full-length Stamp2 back into Stamp2$^{-/-}$ macrophages. As Stamp2 possesses an oxidoreductase domain that may serve an enzymatic function, we also added back an oxidoreductase-deficient mutant form of Stamp2 (Stamp2$^{\Delta N}$). As shown in Fig. 2F, this approach led to comparable expression of either Stamp2 or Stamp2$^{\Delta N}$ in Stamp2$^{-/-}$ macrophages. Furthermore, re-expression of wild-type Stamp2 dampened the LPS-induced pro-inflammatory gene expression in Stamp2$^{-/-}$ cells (Fig. 2G), demonstrating the causal role of Stamp2 for the observed phenotype. In contrast, oxidoreductase-deficient Stamp2$^{\Delta N}$ did not exhibit a similar ability to suppress inflammation (Fig. 2G). Based on these findings, we concluded that the oxidoreductase domain of Stamp2, and the activity it possesses, is critical for Stamp2's ability to dampen inflammation.

Next, we investigated the potential role of the oxidoreductase activity of Stamp2 in the control of the inflammatory response. In fact, the oxidoreductase domain of Stamp2 is a Rossman Fold domain that is largely conserved across species and is predicted to bind to NADPH (Fig. 3A top insert). This raises the possibility that Stamp2 utilizes NADPH for reductive catalysis and may be implicated in the regulation of cellular NADPH homeostasis. Therefore, we measured NADPH levels in Stamp2$^{-/-}$ and WT primary peritoneal macrophages. As shown in Fig. 3A, Stamp2$^{-/-}$ macrophages had significantly higher levels of cellular NADPH compared to WT controls. Given the role of NADPH in inflammatory processes, we then postulated that this excess NADPH availability could be fueling the overt inflammatory phenotype observed in Stamp2 deficiency. To test this hypothesis, we genetically and pharmacologically inhibited the primary NADPH-producing enzyme glucose 6-phosphate dehydrogenase (G6PDx) in Stamp2$^{-/-}$ cells. Chemical inhibition with dehydroepiandrosterone (DHEA) decreased NADPH levels (Fig. S2A), was not cyto- or proteotoxic (Fig. S2B–C), and essentially completely blocked LPS-induced IL-6 expression in Stamp2$^{-/-}$ macrophages (Fig. 3B). To complement the chemical approach, we also targeted G6PDx genetically by RNA interference. This approach resulted in reduced G6PDx both at the mRNA and protein levels (Fig. 3C and Fig. S2D–E), and also significantly reduced LPS-induced IL-6 expression in Stamp2$^{-/-}$ macrophages (Fig. 3D). To assess a direct role for Stamp2 in this regulatory mechanism, we also tested whether we could rescue the elevated NADPH levels in Stamp2$^{-/-}$ macrophages by reconstituting Stamp2 back into these cells. As shown in Fig. 3E, re-expression of WT Stamp2 in Stamp2$^{-/-}$ macrophages caused a significant reduction in NADPH levels, which did not occur when oxidoreductase-deficient Stamp2$^{\Delta N}$ was introduced. These data demonstrate that Stamp2 regulates NADPH levels in macrophages, and this regulatory mechanism may be critical for the control of inflammatory responses.

Next, we examined whether and which inflammatory signaling pathways were altered in Stamp2$^{-/-}$ macrophages and evaluated phosphorylation of the MAP kinases ERK, JNK, and p38. We found increased LPS-induced phosphorylation of p38 in Stamp2$^{-/-}$ cells compared to WT, whereas phosphorylation of ERK and JNK was not altered (Fig. 3F–G and Fig. S2F–G). As p38 activation is frequently associated with increased signaling via NF- κB in immune cells, we also determined phosphorylation of p65. As shown in Fig. 3F–G, LPS induced phosphorylation of p65 to a significantly greater extent in Stamp2$^{-/-}$ cells compared to WT, potentially explaining the pro-inflammatory phenotype. In contrast, there were no differences in TLR4 expression. It has been reported that when cellular NADPH levels are low, the NADPH sensor protein NMRAL1 (NmrA-like family domain-containing protein 1) translocates to the nucleus and targets p65 for degradation and furthermore releases COMMD1 (copper metabolism gene MURR1 domain containing protein 1) to inhibit NF-κB (Lian and Zheng, 2009; Zheng et al., 2007). As this protein may link increased NADPH levels to the pro-inflammatory phenotype, we determined regulation of NMRAL1 in cytosolic and nuclear fractions in Stamp2$^{-/-}$ cells. As shown in Fig. 3H–I, nuclear translocation of NMRAL1 was significantly decreased in LPS-treated Stamp2$^{-/-}$ cells compared to WT controls. These results indicate that Stamp2's anti-inflammatory properties are dependent upon regulation of NADPH metabolism by its oxidoreductase activity which engages inflammatory pathways. Our data also identify at least one potential mechanism of controlling inflammatory signaling through the NADPH sensor protein NMRAL1.

Role of Stamp2 for macrophage foam cell formation

Loading of macrophages with modified lipids may promote foam cell formation and also influence the inflammatory responses. Hence, we assessed expression of IL-6 and TNF-α, as well as NO production, in cells after exposure to oxLDL (Fig. S2H–J) and in this setting Stamp2$^{-/-}$ macrophages also exhibited higher levels of these mediators compared to WT cells. Using thioglycollate elicited primary macrophages we also detected a significant increase of foam cell formation due to Stamp2-deficiency (Fig. S3A–B). We verified these results by loading cells with DiI-labelled oxLDL particles, followed by quantification of fluorescence intensity of the lysates normalized for protein concentration (Devaraj et al., 2001) (Fig. S3C). We also examined the *in vivo* relevance of these observations in an established macrophage transfer model (Li et al., 2004) where thioglycollate-elicited primary macrophages were injected into the peritoneal cavity of ApoE$^{-/-}$ mice kept on Western diet for 6 weeks prior to the experiment. Three days later, macrophages were recovered and stained with Oil Red O. In this setting, foam cell formation of Stamp2$^{-/-}$ macrophages was higher compared to WT cells (Fig. S3D–E), confirming the *in vivo* relevance of our findings. As macrophage inflammation is associated with disturbed cholesterol clearance (Chen et al., 2007; Khovidhunkit et al., 2003), we assessed macrophage efflux of radiolabeled cholesterol. As shown in Fig. S3F, Stamp2$^{-/-}$ macrophages showed decreased cholesterol efflux, and consistent with this phenotype, exhibited a significant decrease in the expression of the ABC transporters ABCA1 (Fig. S3G–I) and ABCG1 (Fig. S4J–L). In contrast, scavenger receptor CD36 and SR-A expression was similar between genotypes (data not shown). These findings show that foam cell formation of Stamp2$^{-/-}$ macrophages was enhanced, most likely due to impaired cholesterol efflux secondary to decreased expression of ABC transporters. Together with the

enhanced inflammatory properties of Stamp2$^{-/-}$ macrophages, these data point towards a potential role of Stamp2 during atherogenesis.

Deficiency of Stamp2 promotes early atherosclerosis in ApoE$^{-/-}$ mice

If macrophage Stamp2 plays a role in atherosclerosis, expression of the protein within the vascular lesion may be anticipated. Indeed, Stamp2 was expressed in both human (Fig. 4A) and mouse (Fig. 4B) atherosclerotic plaques, and expression was co-localized with expression of macrophage markers, supporting a role in lesional macrophages. To analyze the role of Stamp2 in early atherosclerotic lesion formation, we crossed Stamp2$^{-/-}$ mice with the ApoE$^{-/-}$ model. At 6 weeks of age, littermate mice (n=12 Stamp2$^{-/-}$ApoE$^{-/-}$ and n=10 Stamp2$^{+/+}$ApoE$^{-/-}$ mice, respectively) were challenged with Western diet for an additional 6 weeks. On atherogenic diet, there were no statistically significant changes of glucose clearance rates, total serum cholesterol and triglyceride levels, lipid profiles, body weight or blood glucose levels between groups (Fig. S4A–C). Hence, this model serves well to analyze the impact of macrophage contributions independent of systemic metabolic alterations. *En face* analysis demonstrated a 77% increase of atherosclerotic lesion area in the aortas of Stamp2$^{-/-}$ApoE$^{-/-}$ mice compared to Stamp2$^{+/+}$ApoE$^{-/-}$ controls (Fig. 4C–E). Similarly, atherosclerotic lesions in the proximal aortas were larger in Stamp2$^{-/-}$ApoE$^{-/-}$ mice (Fig. 4D and F). In line with our observations in cultured macrophages, lesional inflammation, as assessed by staining for TNF-α and IL-6, was higher in sections from Stamp2$^{-/-}$ApoE$^{-/-}$ mice (Fig. S4D–E), whereas assessment of macrophage cell count/lesion area (not shown), smooth muscle cell staining, and van Giesson staining revealed no significant differences (Fig. S4F). We also measured inflammatory cytokine levels in the serum of both groups and were able to detect TNF-α and CXCL1. While there was no difference in CXCL1 levels between groups, there was a small but statistically significant increase in serum TNF-α levels of Stamp2$^{-/-}$ApoE$^{-/-}$ mice (Fig. S4G). Since the changes are rather minor, our observations support a role for Stamp2 in local, rather than systemic, inflammatory changes in this setting. Taken together, these data support a role for macrophage Stamp2 during atherogenesis.

However, in the whole organism, other cells and tissues may have also contributed to the phenotype. To address this, we performed bone marrow transplantation experiments to assess whether Stamp2 deficiency in bone marrow-derived cells is sufficient to induce early atherosclerosis. We transplanted bone marrow collected from Stamp2$^{-/-}$ApoE$^{-/-}$ mice or from ApoE$^{-/-}$ littermates to lethally irradiated 6-week-old ApoE$^{-/-}$ mice (n=11 and n=12, respectively). After 4 weeks on chow diet post engraftment, recipient mice were challenged with Western diet, and reconstitution with donor bone marrow was verified by the representation of donor alleles (Fig. 4G). There were no significant differences in body weight, blood glucose levels, total serum cholesterol or triglycerides, and lipoprotein distribution between groups (Fig. S4H–I). In the *en face* preparations, the extent of total atherosclerotic lesion area was significantly higher in the mice that received Stamp2$^{-/-}$ApoE$^{-/-}$ bone marrow compared to mice that were reconstituted with ApoE$^{-/-}$ cells (Fig. 4H and J). Furthermore, lesion area in this group was also significantly higher in the histological analysis of proximal aortic sections as confirmed by staining with Oil Red O

and MOMA-2 (Fig. 4I and K). These data indicate an important role of Stamp2 during the development of atherosclerosis through its function in bone marrow-derived cells.

DISCUSSION

In this study, we demonstrate that Stamp2 deficiency results in an aggravated inflammatory response and increased foam cell formation in macrophages and accelerates atherosclerosis *in vivo*. The ability of Stamp2 to regulate inflammatory responses in macrophages is dependent on its NADPH oxidoreductase activity, and chemical or genetic inhibition of primary NADPH-producing enzyme G6PDx can rescue the phenotype caused by Stamp2 deficiency. These findings place Stamp2 in a vital position for cellular NADPH catalysis, which is critical for control of immune responses and may have important implications for human disease. In fact, it has been reported that lower cellular NADPH levels due to mutations in the human G6PDx gene can dampen inflammatory responses in mononuclear cells isolated from these subjects (Sanna et al., 2007), and humans and mice with G6PDx deficiency appear to be protected against atherosclerosis (Cocco et al., 1998; Matsui et al., 2006). We detected Stamp2 expression in macrophages of both mouse and human atherosclerotic plaques. Interestingly, decreased Stamp2 expression is evident in circulating monocytes of humans with cardio-metabolic syndrome, and expression levels were inversely correlated with carotid atherosclerosis (Wang et al., 2010). Hence, as a critical regulator of NADPH metabolism, inflammation, and atherosclerosis, Stamp2 may also play a critical role in human cardiovascular disease in general and promote disease particularly in the context of insulin resistance and diabetes.

Stamp2 serves critical functions at the interface of metabolic and inflammatory pathways through its actions in target cells critical for metabolic and immune regulation. However, there are differences in the function of Stamp2 in adipocytes and macrophages. Notably, ablation of Stamp2 in cultured or primary adipocytes leads to decreased insulin action and glucose transport (Wellen et al., 2007). However, in the experimental model used in the current study, this was not the case in macrophages. In an atherogenic background, systemic glucose tolerance was also not impaired in Stamp2-ApoE double-deficient mice. Although it is possible that ApoE deficiency may have at least partially masked potential Stamp2-related effects, these results indicate a more direct role of Stamp2 in the control of macrophage inflammatory responses in a dyslipidemic environment. This is consistent with earlier observations in another model, where the impact of atherosclerosis has also been independent of the effects of aP2 on systemic insulin action, which acts on both adipocytes and macrophages (Furuhashi et al., 2007; Makowski et al., 2001). It will be interesting to explore the potential cell autonomous effects of Stamp2 on other metabolically critical targets such as hepatocytes or central nervous system in the future.

An important role of Stamp2's oxidoreductase domain was evident for regulation of cellular NADPH levels and inflammatory output of macrophages. These metabolic and immune functions may also have relevance beyond atherosclerosis and influence other disease states such as tumorigenesis. For example, Stamp2 expression is regulated by androgens, and Stamp2 is overexpressed in androgen receptor-positive prostate cancer cell lines where it contributes to increased growth and colony formation (Sendamarai et al., 2008). These

regulatory patterns may also be the result of Stamp2's role in altered cellular metabolism in tumor cells, where proliferating cells may need an increased expression of Stamp2 to meet the increased demand for nutrients. Inflammatory changes are also commonly associated with cancers and influence the progression and outcomes. Whether tumor formation and/or tumor inflammation are also controlled by Stamp2 and whether this molecule contributes to increased tumor incidence seen in obesity remain interesting future areas of investigation. Nonetheless, the function of Stamp2 as a regulatory protein of NADPH homeostasis and inflammatory responses opens up possibilities of its involvement in several pathological settings and indicate that Stamp2 may represent a suitable target for pharmacological intervention targeting cancer, metabolic, or cardiovascular diseases.

EXPERIMENTAL PROCEDURES

Animal studies

Animal care and experimental procedures were performed with approval from animal care committees of Harvard University. Generation of Stamp2$^{-/-}$ and wild-type mice and backcrossing to the C57BL/6 background were performed as described previously (Wellen et al., 2007). Mice homozygous for the inactivation of Stamp2 were intercrossed with ApoE$^{-/-}$ mice also in the C57BL/6 background (Jackson Laboratories) to generate mice heterozygous at both loci. These Stamp2$^{-/+}$ApoE$^{-/+}$ mice were then intercrossed to produce Stamp2$^{-/-}$ApoE$^{-/-}$ mice along with Stamp2$^{+/+}$ApoE$^{-/-}$ littermate controls. Male mice were kept on a 12-hr light/dark cycle and were fed a high-cholesterol atherogenic Western diet (D12079B: 21% fat, 0.21% cholesterol; Research Diets) ad-libitum, beginning at 6 weeks of age. Before and after treatment, blood samples were collected from animals after 6hr of food withdrawal, and the glucose tolerance test was performed by intraperitoneal glucose injection (1.5 g/kg) on conscious mice after overnight (15hr) food withdrawal after 5 weeks of Western diet (7 weeks in bone marrow-transplanted mice).

Bone marrow transplantation (BMT)

Six-week-old recipient mice were lethally irradiated with two 5-Gy doses (total 10 Gy) from a cesium source at a 4-hour interval in order to minimize radiation toxicity. Bone marrow was collected by flushing the femurs and tibiae from sex-matched donor mice (6–8 weeks of age) with phosphate-buffered saline (PBS). Each recipient mouse was injected with 4×10^6 bone marrow cells in 0.2 ml PBS into the retro-orbital venous plexus. During 1 week before and 4 weeks following BMT, 100 mg/L neomycin and 10 mg/L polymyxin B sulfate were added to the drinking water as described (Vallerie et al., 2008).

Assessment of atherosclerosis and immunohistochemistry

Perfusion fixation, preparation of aortas and quantification of atherosclerotic lesions were performed as described (Furuhashi et al., 2007). *En face* pinned aortas were stained with Sudan IV. The heart with the proximal aorta was embedded in OCT (Sakura Finetek) and snap frozen in 2-methylbutane. Lesions in the proximal aorta from serial 8-μm-thick cryosections were stained with Oil Red O and counterstained with haematoxylin. Images of the aortas and immunohistochemistry slides were captured with a digital color camera (DP70; Olympus) mounted on a microscope. All quantitative analysis of images were

performed using ImageJ software and immunohistochemistry was performed as described with the indicated antibodies (Erbay et al., 2009; Furuhashi et al., 2007). Human aortic lesions were collected from 4 male patients, and 1 female patient ages ranging from 57–72, fixed in 10% formalin and paraffin embedded until further processing. At the time of immunostaining, serial sections were de-paraffinized and stained using Stamp2 or CD68 antibody following a citrate buffer epitope retrieval step, and visualized with DAB. Van Giesson and dehydroethidium staining (Zanetti et al., 2005) and biochemical assays were performed as described (Furuhashi et al., 2007).

Examination of macrophage cytokine and nitric oxide production

Supernatants from primary macrophages treated with LPS (Sigma) as indicated were evaluated for the production of IL-6, MCP-1 and TNF-α by ELISA (R&D), and IL-1β by electrochemiluminescence (MesoScale Discovery). The iNOS inhibitor W1400 (Cayman Chemical) was used at a concentration of 10 μmol/L. Supernatants of macrophages treated as described above were evaluated for nitric oxide production utilizing the Griess reaction with a commercial system (Invitrogen). Cytokine and nitric oxide levels were normalized to cellular protein content.

NADPH measurements

The protocol used was adapted from a previous publication (Zhang et al., 2000). Briefly, cells were lysed, and pyridine nucleotides were liberated from cells with two freeze-thaw cycles followed by sonication. After pelleting and removal of cell debris by centrifugation, absorbance was measured using a NanoDrop 2000 (ThermoScientific) at 340nm to measure NADPH+NADH. All of the NADPH was converted to NADP+ using glutathione in the presence of oxidized GSSH, and absorbance was measured at 340nm to determine total NADH. NADPH was calculated by subtracting NADH from NADPH+NADH, and levels were normalized to total protein content.

Statistical analysis

Experimental results are shown as means ± S.E.M. Mean values for biochemical data from each group were compared by Student’s t-test. Data on vascular lesions, which were not normally distributed, were analyzed with a non-parametric Mann–Whitney test. Comparisons between time points were analyzed using repeated-measures analysis of variance, ANOVA. All statistical tests with $p<0.05$ were considered significant.

Supplementary Material

Refer to Web version on PubMed Central for supplementary material.

Acknowledgments

We thank all members of the Hotamisligil lab and Torstein Lindstad from the Saatcioglu lab for scientific input and helpful and inspiring discussions. We thank Lisa Rickey, Megan Washack and Mollie Jurewicz for excellent technical assistance. These studies were supported in part by a grant from the National Institutes of Health (DK52539) to GSH and from Norwegian Research Council and Cancer Society to FS. HtF was supported by the Deutsche Forschungsgemeinschaft (FR 2752/1-1) and the Köln Fortune Program of the University of Cologne

(33/2008). ESC is supported by a training grant from NIH (T32 CA009078), SNV was supported by a fellowship from NIH (F31 DK72556).

REFERENCES

Arner P, Stenson BM, Dungner E, Naslund E, Hoffstedt J, Ryden M, Dahlman I. Expression of six transmembrane protein of prostate 2 in human adipose tissue associates with adiposity and insulin resistance. J Clin Endocrinol Metab. 2008; 93:2249–2254. [PubMed: 18381574]

Chen M, Li W, Wang N, Zhu Y, Wang X. ROS and NF-kappaB but not LXR mediate IL-1beta signaling for the downregulation of ATP-binding cassette transporter A1. Am J Physiol Cell Physiol. 2007; 292:C1493–C1501. [PubMed: 17135302]

Cocco P, Todde P, Fornera S, Manca MB, Manca P, Sias AR. Mortality in a cohort of men expressing the glucose-6-phosphate dehydrogenase deficiency. Blood. 1998; 91:706–709. [PubMed: 9427729]

Devaraj S, Hugou I, Jialal I. Alpha-tocopherol decreases CD36 expression in human monocyte-derived macrophages. J Lipid Res. 2001; 42:521–527. [PubMed: 11290823]

Eguchi K, Manabe I, Oishi-Tanaka Y, Ohsugi M, Kono N, Ogata F, Yagi N, Ohto U, Kimoto M, Miyake K, et al. Saturated Fatty Acid and TLR Signaling Link beta Cell Dysfunction and Islet Inflammation. Cell Metab. 2012

Erbay E, Babaev VR, Mayers JR, Makowski L, Charles KN, Snitow ME, Fazio S, Wiest MM, Watkins SM, Linton MF, et al. Reducing endoplasmic reticulum stress through a macrophage lipid chaperone alleviates atherosclerosis. Nat Med. 2009; 15:1383–1391. [PubMed: 19966778]

Fedorov R, Hartmann E, Ghosh DK, Schlichting I. Structural basis for the specificity of the nitric-oxide synthase inhibitors W1400 and Nomega-propyl-L-Arg for the inducible and neuronal isoforms. J Biol Chem. 2003; 278:45818–45825. [PubMed: 12954642]

Furuhashi M, Tuncman G, Gorgun CZ, Makowski L, Atsumi G, Vaillancourt E, Kono K, Babaev VR, Fazio S, Linton MF, et al. Treatment of diabetes and atherosclerosis by inhibiting fatty-acid-binding protein aP2. Nature. 2007; 447:959–965. [PubMed: 17554340]

Han S, Liang CP, DeVries-Seimon T, Ranalletta M, Welch CL, Collins-Fletcher K, Accili D, Tabas I, Tall AR. Macrophage insulin receptor deficiency increases ER stress-induced apoptosis and necrotic core formation in advanced atherosclerotic lesions. Cell Metab. 2006; 3:257–266. [PubMed: 16581003]

Hotamisligil GS. Inflammation and metabolic disorders. Nature. 2006; 444:860–867. [PubMed: 17167474]

Inoue A, Matsumoto I, Tanaka Y, Iwanami K, Kanamori A, Ochiai N, Goto D, Ito S, Sumida T. Tumor necrosis factor alpha-induced adipose-related protein expression in experimental arthritis and in rheumatoid arthritis. Arthritis Res Ther. 2009; 11:R118. [PubMed: 19660107]

Khovidhunkit W, Moser AH, Shigenaga JK, Grunfeld C, Feingold KR. Endotoxin down-regulates ABCG5 and ABCG8 in mouse liver and ABCA1 and ABCG1 in J774 murine macrophages: differential role of LXR. J Lipid Res. 2003; 44:1728–1736. [PubMed: 12777468]

Li AC, Binder CJ, Gutierrez A, Brown KK, Plotkin CR, Pattison JW, Valledor AF, Davis RA, Willson TM, Witztum JL, et al. Differential inhibition of macrophage foam-cell formation and atherosclerosis in mice by PPARalpha, beta/delta, and gamma. J Clin Invest. 2004; 114:1564–1576. [PubMed: 15578089]

Lian M, Zheng X. HSCARG regulates NF-kappaB activation by promoting the ubiquitination of RelA or COMMD1. J Biol Chem. 2009; 284:17998–18006. [PubMed: 19433587]

Lumeng CN, Saltiel AR. Inflammatory links between obesity and metabolic disease. J Clin Invest. 2011; 121:2111–2117. [PubMed: 21633179]

Makowski L, Boord JB, Maeda K, Babaev VR, Uysal KT, Morgan MA, Parker RA, Suttles J, Fazio S, Hotamisligil GS, et al. Lack of macrophage fatty-acid-binding protein aP2 protects mice deficient in apolipoprotein E against atherosclerosis. Nat Med. 2001; 7:699–705. [PubMed: 11385507]

Matsui R, Xu S, Maitland KA, Mastroianni R, Leopold JA, Handy DE, Loscalzo J, Cohen RA. Glucose-6-phosphate dehydrogenase deficiency decreases vascular superoxide and atherosclerotic lesions in apolipoprotein E(−/−) mice. Arterioscler Thromb Vasc Biol. 2006; 26:910–916. [PubMed: 16439706]

Medzhitov R. Origin and physiological roles of inflammation. Nature. 2008; 454:428–435. [PubMed: 18650913]

Ohgami RS, Campagna DR, McDonald A, Fleming MD. The Steap proteins are metalloreductases. Blood. 2006; 108:1388–1394. [PubMed: 16609065]

Olefsky JM, Glass CK. Macrophages, inflammation, and insulin resistance. Annu Rev Physiol. 2010; 72:219–246. [PubMed: 20148674]

Sanna F, Bonatesta RR, Frongia B, Uda S, Banni S, Melis MP, Collu M, Madeddu C, Serpe R, Puddu S, et al. Production of inflammatory molecules in peripheral blood mononuclear cells from severely glucose-6-phosphate dehydrogenase-deficient subjects. J Vasc Res. 2007; 44:253–263. [PubMed: 17361089]

Schenk S, Saberi M, Olefsky JM. Insulin sensitivity: modulation by nutrients and inflammation. J Clin Invest. 2008; 118:2992–3002. [PubMed: 18769626]

Sendamarai AK, Ohgami RS, Fleming MD, Lawrence CM. Structure of the membrane proximal oxidoreductase domain of human Steap3, the dominant ferrireductase of the erythroid transferrin cycle. Proc Natl Acad Sci U S A. 2008; 105:7410–7415. [PubMed: 18495927]

Shoelson SE, Lee J, Goldfine AB. Inflammation and insulin resistance. J Clin Invest. 2006; 116:1793–1801. [PubMed: 16823477]

Vallerie SN, Furuhashi M, Fucho R, Hotamisligil GS. A predominant role for parenchymal c-Jun amino terminal kinase (JNK) in the regulation of systemic insulin sensitivity. PLoS One. 2008; 3:e3151. [PubMed: 18773087]

Wang ZH, Zhang W, Gong HP, Guo ZX, Zhao J, Shang YY, Feng JB, Zhang Y, Zhong M. Expression of STAMP2 in monocytes associates with cardiovascular alterations. Eur J Clin Invest. 2010

Wellen KE, Fucho R, Gregor MF, Furuhashi M, Morgan C, Lindstad T, Vaillancourt E, Gorgun CZ, Saatcioglu F, Hotamisligil GS. Coordinated regulation of nutrient and inflammatory responses by STAMP2 is essential for metabolic homeostasis. Cell. 2007; 129:537–548. [PubMed: 17482547]

Zanetti M, d'Uscio LV, Peterson TE, Katusic ZS, O'Brien T. Analysis of superoxide anion production in tissue. Methods Mol Med. 2005; 108:65–72. [PubMed: 16028676]

Zhang Z, Yu J, Stanton RC. A method for determination of pyridine nucleotides using a single extract. Anal Biochem. 2000; 285:163–167. [PubMed: 10998277]

Zheng X, Dai X, Zhao Y, Chen Q, Lu F, Yao D, Yu Q, Liu X, Zhang C, Gu X, et al. Restructuring of the dinucleotide-binding fold in an NADP(H) sensor protein. Proc Natl Acad Sci U S A. 2007; 104:8809–8814. [PubMed: 17496144]

HIGHLIGHTS

- Stamp2 regulates NADPH metabolism and inflammatory responses in macrophages.
- Stamp2's oxidoreductase domain is critical for control of the inflammatory responses.
- Stamp2 deficiency promotes foam cell formation due to reduced cholesterol efflux.
- Total body or myeloid Stamp2 deficiency in mice promotes atherosclerosis.

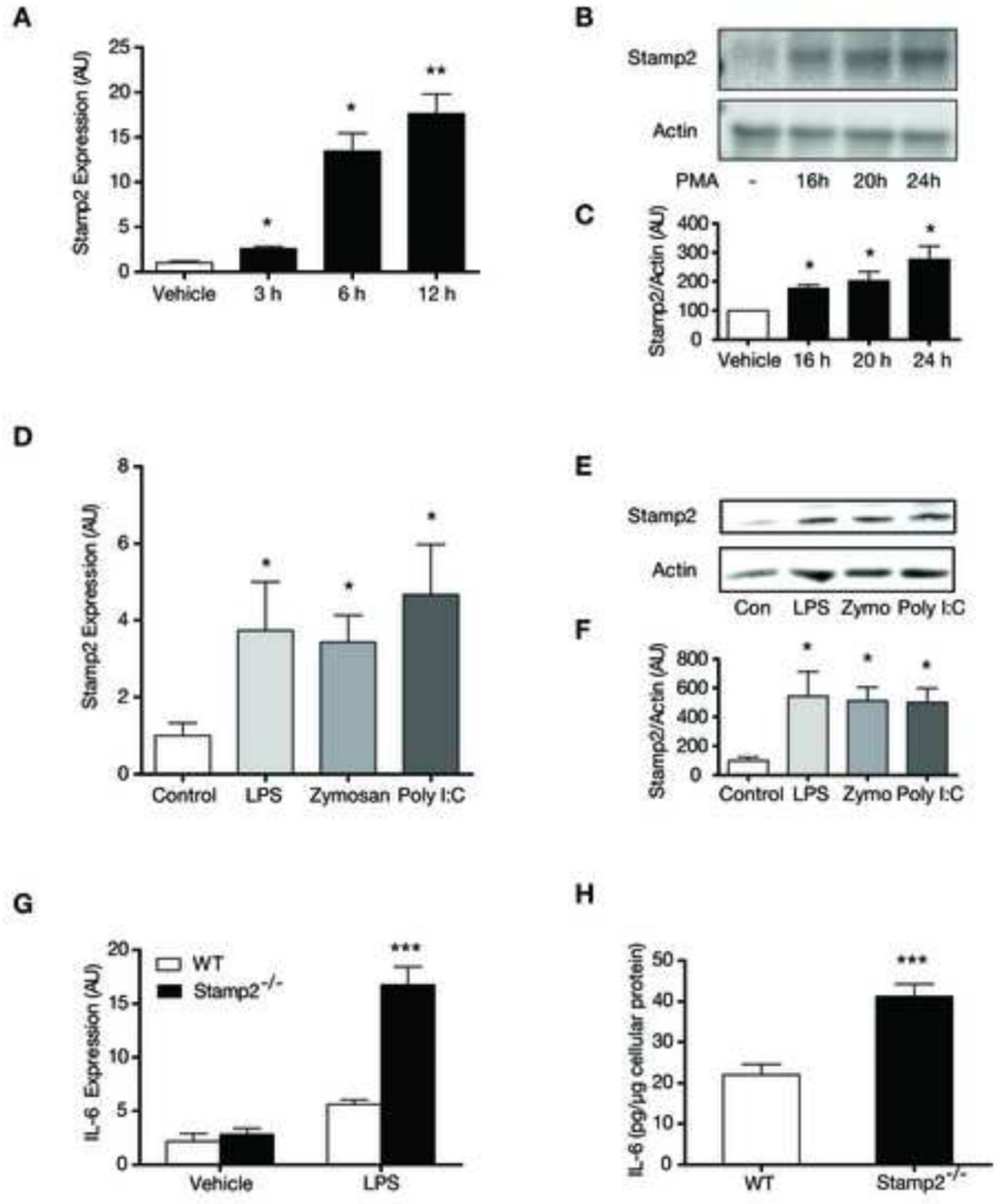

Figure 1. Expression and regulation of Stamp2 in macrophages

Human THP-1 monocytes were treated with 100 ng/mL PMA or vehicle for indicated time points followed by assessment of Stamp2 mRNA (A) or protein expression (B–C) (n=4–5). Primary peritoneal macrophages were treated with LPS (100 ng/mL), Zymosan (50 µg/mL), or Poly I:C (50 µg/mL) followed by evaluation of Stamp2 mRNA (D) or protein expression (E–F) (n=4–5).

IL-6 mRNA expression was assessed in primary WT and Stamp2$^{-/-}$ macrophages at baseline and after treatment with LPS (10 ng/mL for 24hr) (G) (n=6–8).

(H) IL-6 secretion into the culture medium by cells treated as in (G) was measured and normalized to cellular protein content (n=9–12). Data are presented as means±SEM. *p<0.05, **p<0.01, ***p<0.001 in Student's t-test.

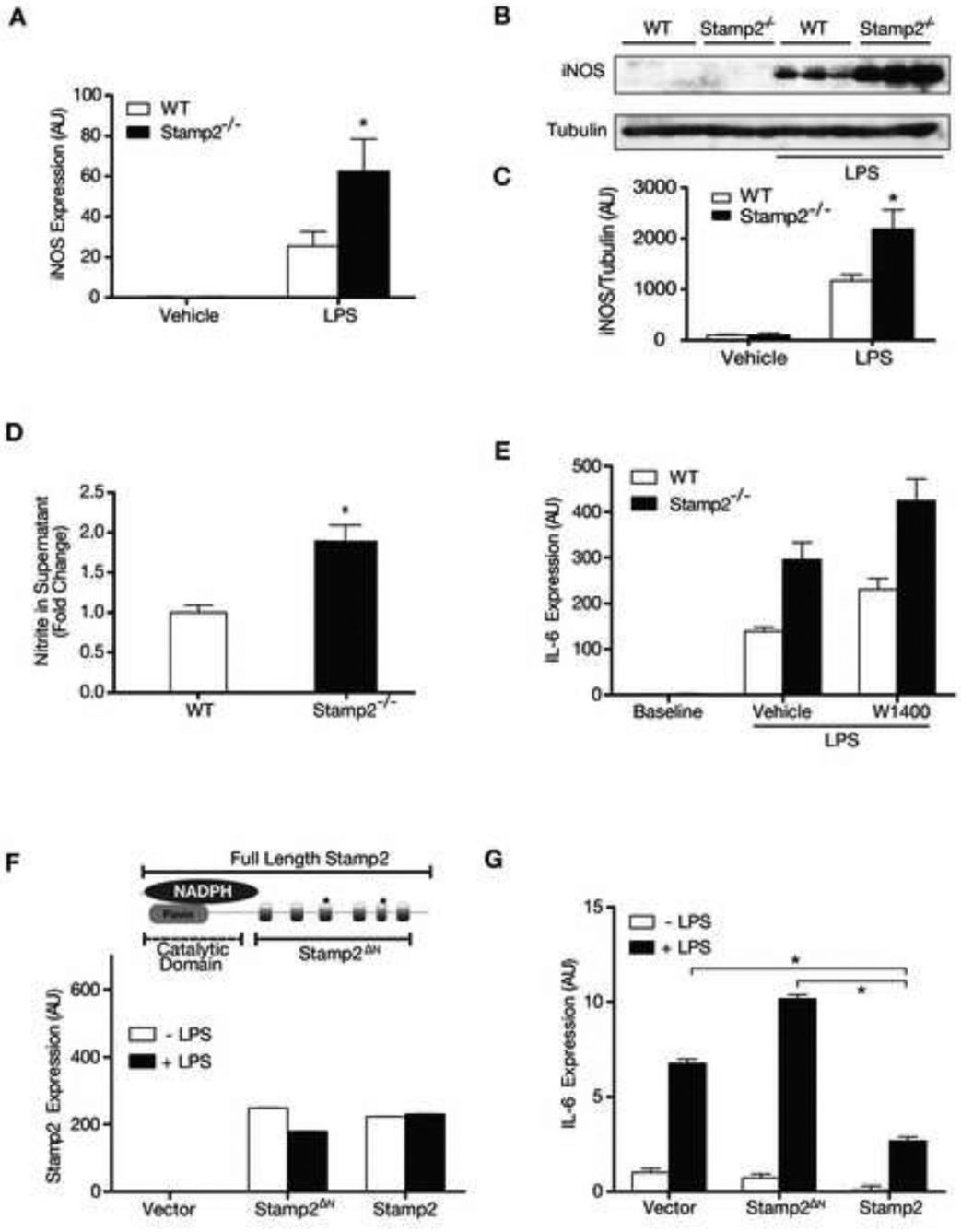

Figure 2. Regulation of iNOS expression and NO production by Stamp2

Expression of iNOS was detected at the mRNA (A) and protein level (B–C) in primary WT and Stamp2$^{-/-}$ macrophages treated with LPS (10ng/mL for 24hr) (n=6–10).

(D) NO production was measured in culture medium from cells treated with LPS (10 ng/mL) for 24hr normalized for cellular protein content (n=11).

Primary peritoneal macrophages were treated with the iNOS inhibitor W1400 (10 μM) and 2hr later stimulated with LPS (100 ng/mL for 4hr) followed by assessment of IL-6 mRNA expression (E) (n=4).

(F)Primary Stamp2$^{-/-}$ acrophages were electroporated with Stamp2-expressing vector, catalytic domain-deficient Stamp2 expressing-vector (Stamp2$^{\Delta N}$) or control plasmids (mutant depicted in the top panel). (G)IL-6 mRNA expression is shown after LPS (100ng/mL for 4hr) treatment following electroporation with vectors mention in (F) (n=3). Data are presented as means±SEM, *p<0.05 in Student's t-test.

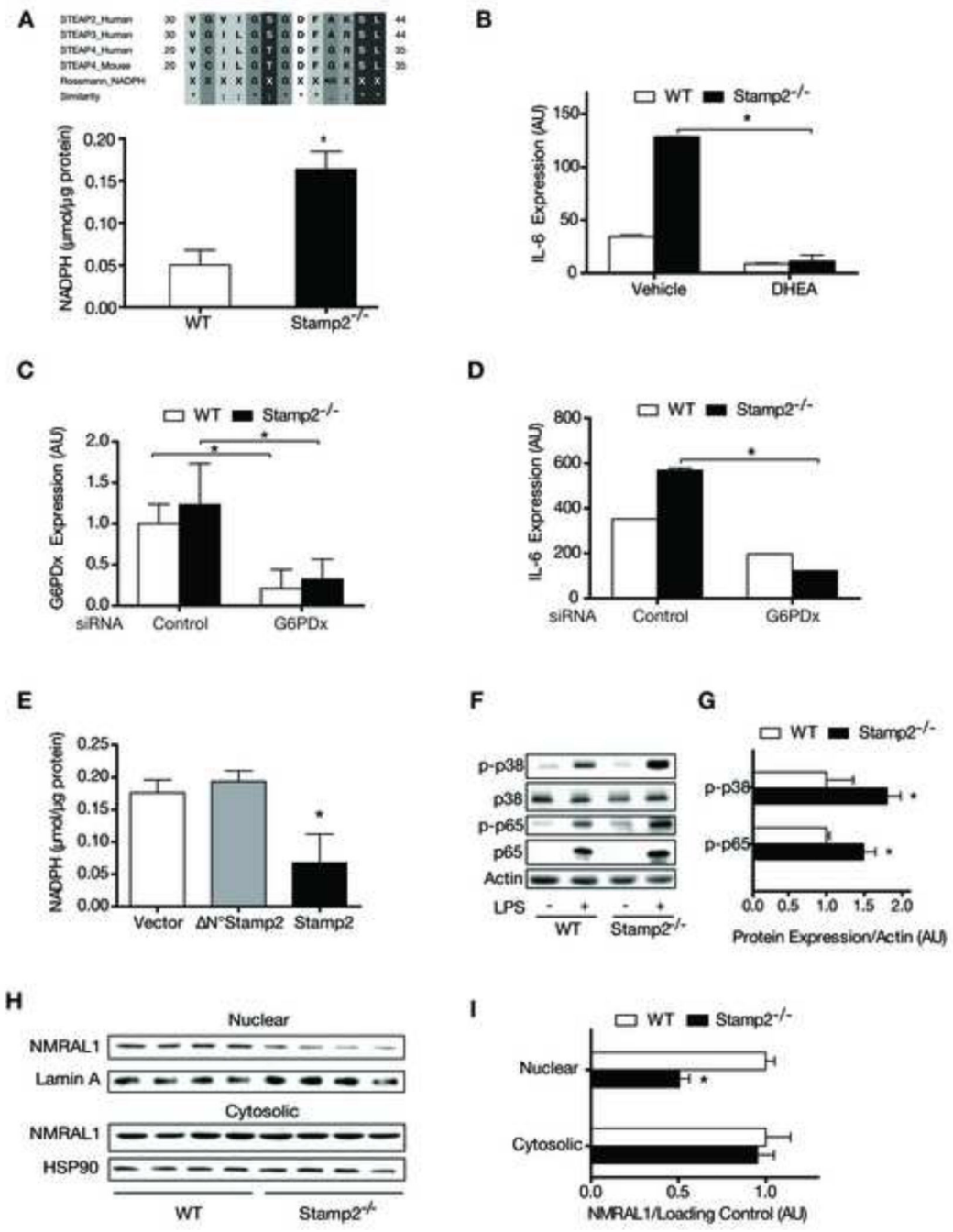

Figure 3. NADPH-dependent regulation of inflammatory responses by Stamp2 in macropages

NADPH levels were measured in Stamp2$^{-/-}$ and WT primary peritoneal macrophages (A). Homology of STAMP family members with NADPH binding Rossman Fold domain is depicted in the top panel.

G6PDx was inhibited in primary peritoneal macrophages by 50μM DHEA followed by LPS treatment (100 ng/mL) and assessment of IL-6 mRNA expression (B). RNA interference directed against G6PDx gene resulted in >70% knock down of the gene (C). IL-6 mRNA

expression was assessed 24hr after siRNA-induced knock down of G6PDx and after LPS treatment (D) (n=3).

Primary peritoneal macrophages from Stamp2$^{-/-}$ mice were electroporated as in Fig. 2E-F, followed by analysis of NADPH levels (E) (n=4–5).

Primary peritoneal macrophages were treated with LPS or vehicle followed by western blot analyses of the expression of phosphorylated and total proteins (F–G).

Cell lysates as in (F) were used to prepare nuclear and cytosolic fractions followed by western blot analyses of NMRAL1 expression and Lamin A/HSP90 expression as loading controls (H–I) (n=4). Data are presented as means±SEM, *p<0.05, in Student's t- test.

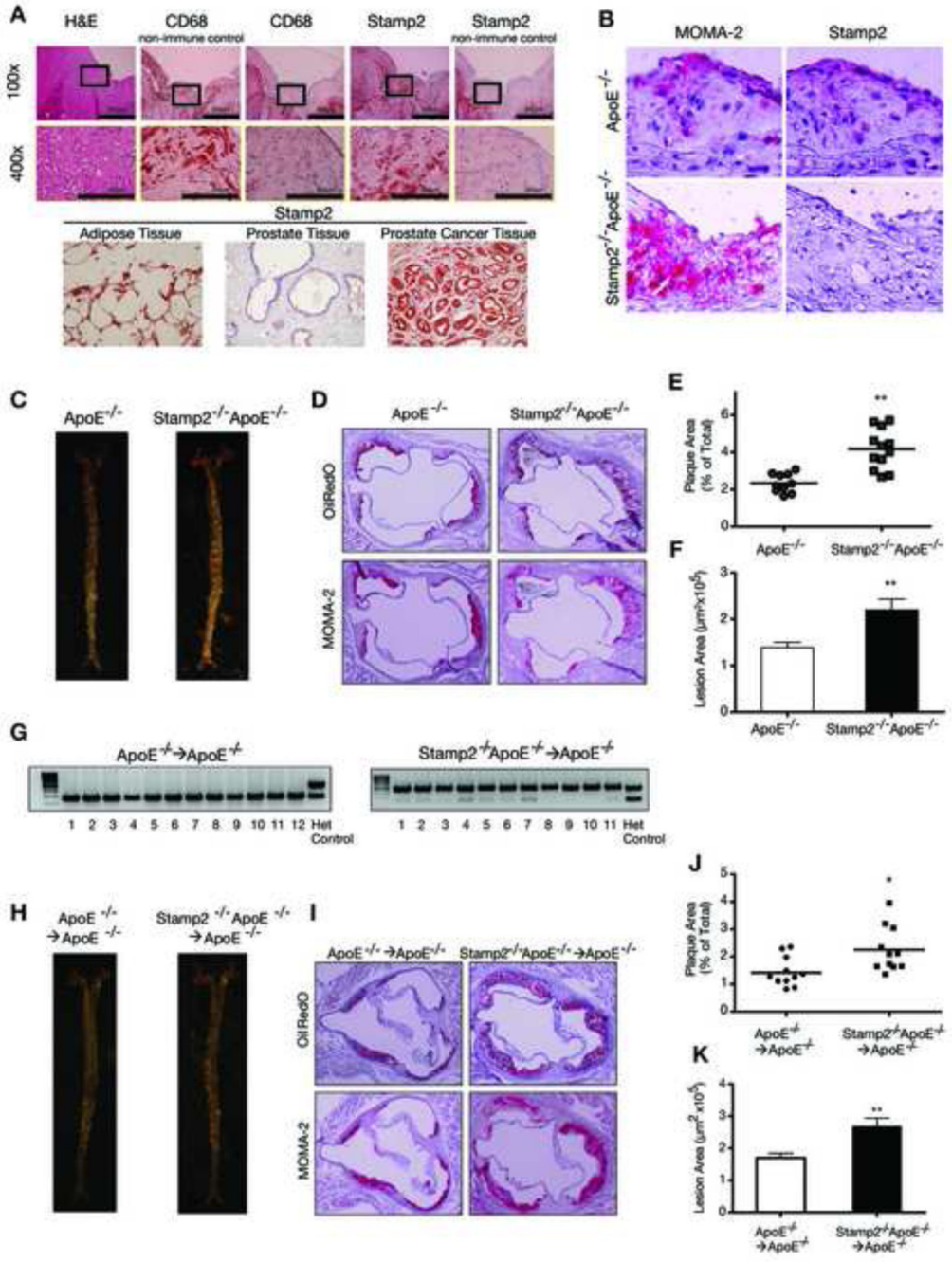

Figure 4. Regulation of atherosclerotic lesion formation in total body or bone-marrow Stamp2 deficiency

(A)H&E stainings along with non-immune controls for CD68 and Stamp2 of human atherosclerotic plaques are shown, Below, Stamp2 staining of tissues with known high expression of Stamp2 (adipose tissue, prostate tissue, prostate cancer tissue) are presented to further support specificity of the antibody. Representative MOMA-2 and Stamp2 immunohistochemistry stainings of murine atherosclerotic plaques from $ApoE^{-/-}$ (top panel) and $Stamp2^{-/-}ApoE^{-/-}$ mice (as staining controls, bottom panel) (B).

Representative Sudan IV-stained pinned *en face* aortic preparations (C) and aortic root sections (D) stained with Oil Red O, and staining with MOMA-2 was performed on $ApoE^{-/-}$ and $Stamp2^{-/-}ApoE^{-/-}$ mice after 6 weeks of Western diet (C). Quantification of atherosclerotic plaque area in *en face* preparations (E) and plaque area in the aortic root sections (F) (n=8–12). Genotyping results of blood from $ApoE^{-/-} \rightarrow ApoE^{-/-}$ and $STAMP2^{-/-}$ $ApoE^{-/-} \rightarrow ApoE^{-/-}$ mice together with a tail DNA sample from a $Stamp2^{+/-}$ mouse as control ("Het Control"). The upper band depicts the $Stamp2^{-/-}$ allele, whereas the lower band represents the WT allele (G). Representative Sudan IV-stained pinned out *en face* preparations of aortas from $ApoE^{-/-} \rightarrow ApoE^{-/-}$ and $Stamp2^{-/-}ApoE^{-/-} \rightarrow ApoE^{-/-}$ mice after 8 weeks of Western diet (H), and representative aortic root sections (I) stained with Oil Red or staining with MOMA-2 antibody. Quantification of atherosclerotic plaque area in *en face* preparations (J) and plaque area in the aortic root sections (K) (n=8–12). Data are presented as means±SEM, $*p<0.05$, $**p<0.01$ in Mann-Whitney test.